processes

MDPI

Article

Study on the Coalescence-Induced Jumping of Droplets with Different Radii on Superhydrophobic Surface

Ming-Jun Liao, Xin-Quan Ren, Zi-Han Liu, Wen-Peng Hong and Fang-Fang Xie *

School of Energy and Power Engineering, Northeast Electric Power University, Jilin 132012, China; liaomj@neepu.edu.cn (M.-J.L.); rxq2692144252@163.com (X.-Q.R.); lzh_20001205@163.com (Z.-H.L.); hwp@neepu.edu.cn (W.-P.H.)
* Correspondence: xiefang705@163.com

Abstract: The phenomenon of droplet coalescence and jumping has received increasing attention due to its potential applications in the fields of condensation heat transfer and surface self-cleaning. Basic research on the process and mechanism of coalescence-induced droplet jumping has been carried out, and some universal laws have been established. However, it is found that the focus of these studies is based on two identical droplets, and the coalescence-induced jumping with different radii is rarely investigated, which is commonly encountered in nature. Therefore, it is essential to proceed with the research of coalescence and jumping of droplets with unequal radii. In this paper, molecular dynamics (MD) simulations are performed to reveal the effects of radius ratio and radius of small droplets on jumping velocity. The results show that as the increasing of radius ratio with an unchanged small droplet radius of 8.1 nm, the jumping velocity increases then decreases, which indicates there is an optimal radius ratio to maximize the jumping velocity. Additionally, it is found that if the small droplet radius is changed, the critical radius ratio for characterizing whether the coalesced droplet jumping increases with increasing the small droplet radius. Furthermore, according to energy conservation, the conversion efficiency of energy is discussed. The results show that when the radius ratio is greater than 1.3 with three different small droplet radii, the energy conversion efficiency rapidly decreases to below 1.0%; and the critical radius ratios are consistent with the result obtained from the velocity analysis. This work broadens the understanding of the more general phenomenon of coalescence-induced droplet jumping and can better guide industrial applications.

Keywords: coalescence-induced jumping; molecular dynamics simulations; unequal radii; superhydrophobic surfaces; critical radius ratio

Citation: Liao, M.-J.; Ren, X.-Q.; Liu, Z.-H.; Hong, W.-P.; Xie, F.-F. Study on the Coalescence-Induced Jumping of Droplets with Different Radii on Superhydrophobic Surface. *Processes* **2023**, *11*, 1865. https://doi.org/10.3390/pr11071865

Academic Editor: Jan Zawała

Received: 16 May 2023
Revised: 13 June 2023
Accepted: 16 June 2023
Published: 21 June 2023

1. Introduction

Coalescence-induced droplet jumping can effectively remove condensate droplets in a timely manner, which enhances condensation heat transfer efficiency [1,2]. In addition, it plays an important role in applications for self-cleaning [3–5], anti-dew [6], and anti-icing [7,8]. Boreyko et al. [9] are the first group to show that the coalescence of two droplets can spontaneously induce jumping on the superhydrophobic surface with low adhesion in the experiment. The reason for this phenomenon is that the liquid droplets generate excess surface energy during the coalescence process, which overcomes viscous dissipation and adhesion work, converting into upward kinetic energy of the coalesced droplets. Subsequently, the coalesced droplet jumps off the solid surface successfully.

For the phenomenon of coalescence-induced droplet jumping, the methods of experiment [10–15], theory [16–19], and simulations [20–24] are employed to study it in depth. Xie et al. [12] fabricated a nanostructured superhydrophobic surface with tapered nanogaps experimentally, solving the contradiction between nucleation and droplet self-removal. Wang et al. [17] theoretically deduced an expression of the jumping velocity of the coalesced droplet from the energy balance equation and indicated that there is an optimal

droplet radius when the jumping velocity reaches its maximum value. Farokhirad et al. [20] demonstrated the minimum diameter that can cause the coalescing droplets to jump is different for superhydrophobic surfaces with distinct contact angles. Moreover, only 6% of the surface free energy is converted into kinetic energy during the droplet merging process, due to the influence of internal fluid dynamics. Liang et al. [23] and Xie et al. [24] simulated the droplet coalescing process at the nanoscale by molecular dynamics (MD) simulations. They verified the coalesced droplet can jump off the substrate, which cannot be observed in the experiment for the reason that smaller droplets may become embedded into the microstructure on superhydrophobic surfaces, forming a larger contact angle that prevents them from jumping. In general, the jumping velocity of coalesced droplets within a specific radius range gradually decreases with increasing the droplet radius and follows an inertial-capillary scaling law, that is, the dimensionless jumping velocity $v^* = v_j/u_{ic}$ is approximately constant at 0.2 for microscale droplets [17,25] and 0.127 for nanoscale droplets [23,24], where v_j is the measured jumping velocity, and $u_{ic} = (\sigma_l/\rho R)^{1/2}$ is the inertial-capillary velocity, σ_l is the surface tension, ρ is the density, and R is the droplet radius.

The above studies were based on the coalescence of two droplets with equal radius, while unequal-sized droplet merging and jumping commonly took place in nature. The process and mechanism of coalescence-induced jumping in this circumstance are the same as those with equal radius that need to be studied. Therefore, some groups have noticed this problem and paid attention to droplets merging with unequal radii. Liu et al. [26] experimentally concluded that the coalesced droplet will not jump when the size of the two coalescing droplets has a big difference. However, the reason for not jumping is not explained, and the critical radius ratio of large droplets to small droplets when not jumping also cannot be vanished. In this paper, the MD simulations are first performed to investigate the coalescence and jumping process of droplets with equal radius, the purpose of which is to proceed with the model validation. Subsequently, coalescence-induced jumping with unequal-sized droplets is simulated. During this process, the data of jumping velocity is observed, and its curve is plotted. Through the investigation of jumping velocity, the critical radius ratio is put forward and the law of energy conversion is illustrated. For the first time, this study performs MD simulations to reveal the reason for not jumping two droplets with different radii. It can be attributed to the viscous force, who dominates the coalescence and jumping with large radius ratios. Additionally, this work also provides the critical radius ratio, above which the coalesced droplet will not jump, and further proves the variation trend of the critical radius ratio with the radius of the small droplet. I believe these findings can deepen our understanding of the jumping mechanism with unequal-sized droplets and lay the foundation for establishing a theoretical formula for the critical radius ratio. Furthermore, this also provides a theoretical basis for improving condensation heat transfer efficiency.

2. Model and Validation

Firstly, in order to reproduce the simulation process of reference [23], the following settings are made, as shown in Figure 1. The three-dimensional simulation system consists of gaseous argon, argon droplets, and solid gold plate. The dimension of the simulation cell is 68.4 nm × 44.2 nm × 37.2 nm, where periodic boundary conditions are used in the xyz directions. At the bottom of the system is a solid gold plate with a thickness of 10.24 Å, which is arranged in a face centered cubic lattice structure (FCC) with a lattice constant of 4.08 Å. Throughout the simulation process, the bottom atomic layer of the solid gold plate is fixed to prevent deformation and placed at z = 0 nm, while the upper atomic layers remains at a constant temperature of 85 K under the action of thermostat. Actually, similar treatment was extensively adopted in previous MD studies associated with coalescence-induced jumping phenomena. For example, in Liang et al.'s MD study [23], a flat gold substrate was also employed. For fair comparison, gold plate is thereby also applied in the present simulations. Two solid argon spheres of equal size with a radius of 11.1 nm are placed on the gold plate, whose lattice constant is 5.4 Å and droplet spacing is 4 Å. It

should be noted that although coalescence-induced jumping of water droplets has been extensively investigated in the previous studies; however, owing to the polar interactions between water molecules, an extremely time-consuming computation is required by MD simulations to model water droplets. Furthermore, our preliminary test shows that on a flat gold surface with contact angle of 180°, the jumping velocity is v_j = 0.127 u_{ic} for two water droplets with equal radius of 3.5 nm, indicating that the dimensionless jumping velocity, v_j/u_{ic}, also follows the inertial-capillary scaling law. Therefore, the dimensionless jumping velocity is independent of the fluid type, but only depends on the Ohnesorge number and the contact angle between fluid and substrate. Thus, to save computational cost, argon droplets are chosen in this work.

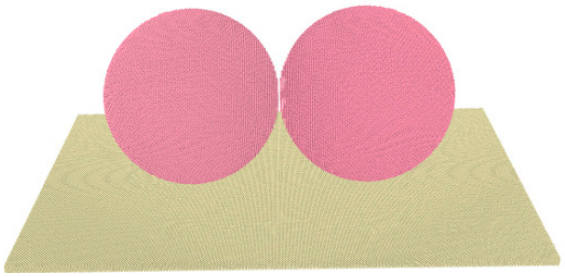

Figure 1. Initial configuration of two identical argon droplets coalescing with a radius of 11.1 nm on a gold plate.

Here, the Ohnesorge number also should be paid some attention. As we have redefined in our previous paper [24], for two unequal sized droplets, the Ohnesorge number can be rearranged as

$$\mathrm{Oh}^* = \frac{\gamma}{\sqrt{\frac{\rho\sigma_1(R_s+R_l)}{2}}} = \frac{\gamma}{\sqrt{\rho\sigma_1 R_s}} \cdot \sqrt{\frac{2}{1+R^*}} = \mathrm{Oh} \cdot \sqrt{\frac{2}{1+R^*}}, \quad (1)$$

where we use Oh* to denote the Ohnesorge number of two unequal sized droplets, while Oh is the Ohnesorge number of two equal sized droplets. Apparently, when R^* = 1, Oh* reduces to the original Ohnesorge number or Oh* = Oh. With the L-J interaction potential, the surface tension, density, and viscosity of liquid argon is σ_1 = 8.16 ± 0.04 mJ m^{-2}, ρ = 1.31 × 10^3 kg m^{-3}, and γ = 190 ± 1 μPa s [23,24], respectively. Thus, the Ohnesorge number for this case is Oh = $\gamma/(\rho\sigma_1 r)^{0.5}$ = 0.55. For the Oh numbers referred to in the third section, they can be calculated using Formula (1).

The interaction force between gold–gold is calculated by using the embedded atom model (EAM) potential [27], while the interaction force between argon–argon and gold–argon is calculated by using the Lennard–Jones 12-6 potentials, expressed as

$$V_{ij} = 4\varepsilon\left[(\sigma/r)^{12} - c_{ij}(\sigma/r)^6\right], \quad (2)$$

where V_{ij} donates the potential energy between particles, r represents the distance between particles, c_{ij} is an energy parameter to characterized intrinsic contact angle between gold and argon, σ and ε are the particle spacing when the potential is zero and the minimum value of the potential, respectively, whose values are 3.14 Å and 10.3 meV in this paper [23]. It should be noted that, c_{ij} can be adjusted to achieve different contact angles and surface adhesion (more details will be described in next paragraph), and the maximum value of c_{ij} is 1, which represents the interaction between argon and argon.

After the preparation of the initial configuration and interaction force field, the energy minimization of the system is carried out first, and then two argon droplets and the gold plate are equilibrated in a canonical (NVT) ensemble at T = 85 K. It should be noted that the NVT ensemble means we can obtain positions and velocities of each atom by performing time integration on Nose–Hoover style non-Hamiltonian equations of motion, in which the number of atoms, volume, and temperature of the system are fixed. To prevent droplets

from detaching from the gold plate, the interaction coefficient c_{ij} of gold–argon is first set to 0.3, and the system is operated for 5 ns to maintain gas–liquid coexistence. Subsequently, gradually adjusting the value of c_{ij} to 0.2 and running for another 10 ns to achieve a contact angle of 180 between the droplet and the plate. Finally, turning off the thermostat, and running for 6 ns in a microcanonical (NVE) ensemble to eliminate the vibration of the droplets and achieve the final equilibrium state, where the NVE ensemble means fixing the number of atoms, volume, and energy of the system.

The evolution of the vertical velocity v_z during the merging process for two identical droplets with a radius of 11.1 nm is shown in Figure 2, where v_z refers to the centroid velocity by averaging five velocities at the moment of $t - 2\Delta\tau$, $t - \Delta\tau$, t, $t + \Delta\tau$, and $t + 2\Delta\tau$ with $\Delta\tau$ = 120 fs. The coalescence process is studied in five stages, which coincides with that in Ref. [23]. Here, the first stage is the process of two droplets approaching each other from adjacent states to contact (0 ps~680 ps), during which the droplet vertical velocity changes around 0, mainly caused by the internal thermal motion of the droplets.

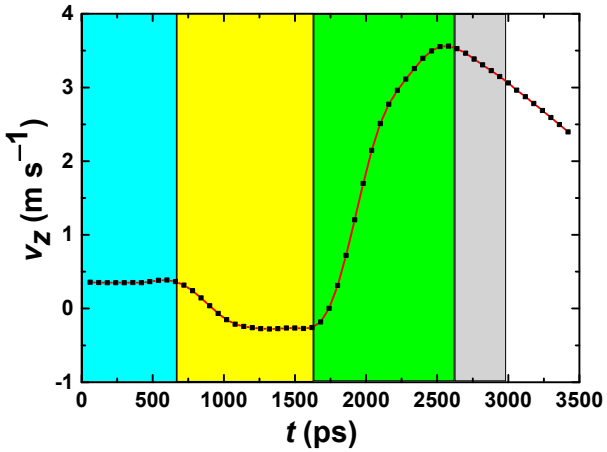

Figure 2. Evolution of vertical velocity of two identical droplets coalescing with a radius of 11.1 nm.

The second stage is the process where the droplets begin to coalesce with each other, and the liquid bridge gradually increases (680 ps~1626 ps). Because the impact of the liquid bridge on the superhydrophobic surface is the primary reason for droplet jumping, this paper accurately captures the variation process of the liquid bridge width and obtains the linear relationship between r_b/R and $(t/\tau)^{1/2}$. The scaling law can be expressed as $r_b/R = C_b(t/\tau)^{1/2}$, as shown in Figure 3, where r_b is the width of the liquid bridge, R is the radius of droplet, C_b is a constant [28,29], t is the moment when two droplets begin to contact each other, and τ is the inertia time of the merging process. The errors depicted in Figure 3 are due to the uncertainty in determining r_b, denoting one standard deviation. According to the calculation, the magnitude of the slope is 0.92 ± 0.02 (Figure 3), which accords with the scaling law and hence further verifies the correctness of the model in this paper.

The third stage is the process of the liquid bridge gradually increasing and impacting the superhydrophobic surface (1626 ps~2544 ps). In the next stage, the coalesced droplet gradually detaches from the substrate (2544 ps~2980 ps), where the vertical velocity v_z rapidly increases to its maximum value and the coalesced droplet is close to spherical. The fifth stage is the process of the coalesced droplet continuing to move upwards and jump away from the superhydrophobic surface (2980 ps~3452 ps), in which the droplet needs to overcome the Stokes resistance of gas phase molecules and the vertical velocity gradually decreases.

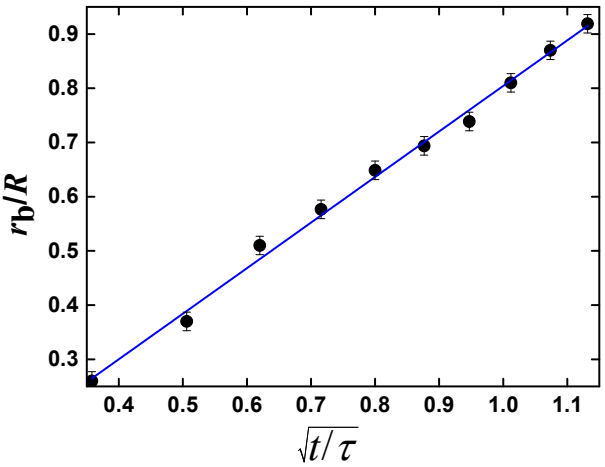

Figure 3. Evolution of normalized bridge width for two identical droplets coalescing with a radius of 11.1 nm. Error bars, denoting one standard deviation.

3. Results and Discussion

3.1. Dynamic Coalescence and Jumping of Two Unequal Sized Droplets

In order to study the jumping velocity characteristics with unequal-sized droplets during the coalescence and jumping process, the radius of the small droplet is set to be R_s = 8.1 nm, and the radius of the large droplet R_l is set to be 8.1 nm, 8.9 nm, 10.0 nm, 12.0 nm, and 16.2 nm, respectively. The evolution of vertical velocity v_z at five different radius ratios was extracted, as shown in Figure 4. It can be seen from Figure 4 that there are some differences in the velocity fluctuation of the first two stages; however, the trends of droplet velocity with five different radius ratios in the other stages are basically consistent. According to observing the process of coalescence-induced droplet jumping, first, the two droplets approach each other and form a liquid bridge after contact. Subsequently, the width of the liquid bridge gradually grows and collides with the bottom metal plate, causing an upward reaction generated from the substrate. Finally, the coalesced droplet jumps off the surface (more details can be seen in Ref. [24]). This indicates that the mechanism of droplet merging and jumping processes with different radius ratios is the same, which can be concluded as the "liquid bridge impacting substrate" mechanism. It can also be found from Figure 4 that in the velocity-increasing stage, when the radius ratio is large, the slope of the increase in velocity is small, which is due to the fact that the influence of liquid bridge impacting the condition of the larger radius ratio is weakened, making the reaction force of the substrate is reduced. Furthermore, when the velocity reaches its maximum value, it begins to decrease, indicating that the velocity is beginning to enter a decreasing stage. The reason for the reduction in velocity is due to the adhesive force between the substrate and the droplet. With increasing the radius ratio of two coalescing droplets, the effect of adhesion force is decreasing. Therefore, the slopes of the vertical velocity in the fourth stage in Figure 4 gradually decrease, and the jumping velocity also decreases accordingly. However, it should be noted that the jumping velocity gradually decreases only when the radius ratio surpasses 1.23. In the range between 1 and 1.23, the jumping velocity gradually increases instead, indicating the existence of an optimal radius ratio that can maximize the jumping velocity. At the same time, when the radius ratio exceeds a certain range, it will suppress the merging and jumping of droplets until there is no longer jumping after merging.

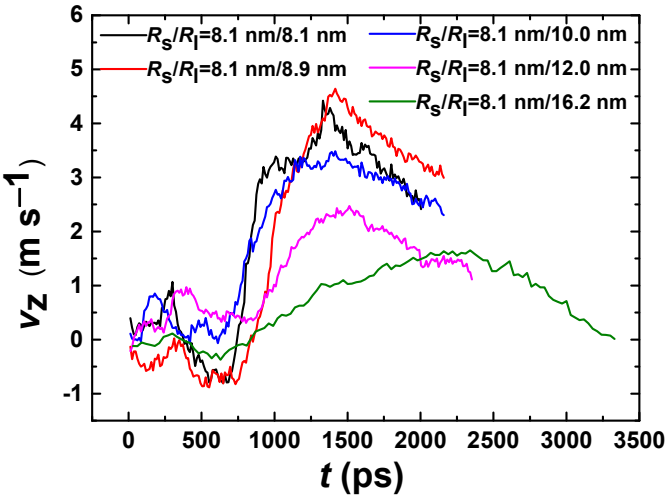

Figure 4. Evolutions of vertical velocity for two unequal-sized droplets coalescing with the radius of small droplet R_s = 8.1 nm, while the radius of large droplet R_l is 8.1 nm, 8.9 nm, 10.0 nm, 12.0 nm and 16.2 nm, respectively.

After clarifying the relationship between the droplet jumping process and the radius ratio, this work further investigates the relationship between the jumping ability of two unequal-sized droplets and the radius of the small droplet. Three simulation series were set up in this paper. The first group is unchanged R_s = 7.5 nm, with R_l ranging from 7.5 nm to 20.0 nm; the second group is unchanged R_s = 8.1 nm, with R_l ranging from 8.1 nm to 22.0 nm; the last group is unchanged R_s = 9.3 nm, with R_l ranging from 9.3 nm to 28.0 nm. The evolutions of coalescence-induced droplet jumping velocity v_j with radius ratio for three series are shown in Figure 5, where v_j refers to the velocity at the moment of the coalesced droplet jumping. It can be seen that for the three groups, as the radius ratio increases, the jumping velocity curves show a similar variation trend. At the initial stage of increasing the radius ratio, there is a slight increase in jumping velocity. That is to say, there exists an optimal radius ratio that maximizes the jumping velocity. While the optimal radius ratios for small droplets with different radii vary slightly, which basically remain stable at 1.23. However, as the radius ratio further increases, the jumping velocity rapidly decreases before the radius ratio is less than 1.5, which is because the deformation of the liquid bridge formed by large and small droplets is relatively large, causing the area of the liquid bridge impacting the solid surface rapidly decreases. In addition, when the radius ratio is greater than 1.5, the descent rate of jumping velocity gradually slows down until the end of the droplet merging and jumping process. From Figure 5, it can be found in the radius ratio increases to a certain extent, the jumping velocity of the merged droplet is basically 0, indicating that no jumping occurs anymore. It should be noted that the critical radius ratios for the three series in this article are R_l/R_s = 2.5, 2.7, and 3, respectively. Therefore, as the radius of small droplets increases, the critical radius ratio for coalescence and jumping gradually increases.

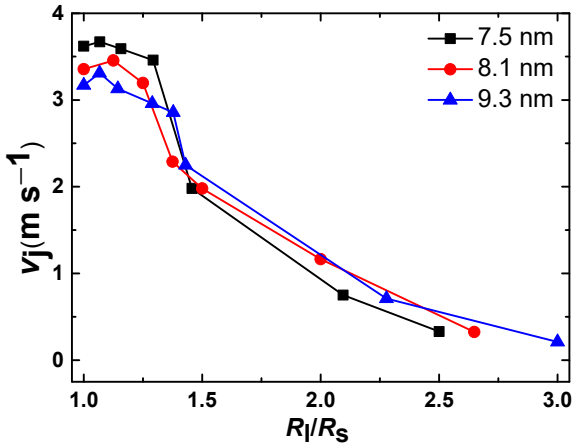

Figure 5. Evolution of jumping velocity with radius ratio for three series.

3.2. Energy Analysis

From the analysis of the morphological changes in the process of droplet coalescence and jumping, the jumping mechanism is based on the theory of the "liquid bridge impacting substrate". On the other hand, from an energy perspective, the occurrence of coalescence-induced droplet jumping is caused by energy conversion of surface energy released during the merger process into kinetic energy of the droplet's upward movement. However, most of the energy is dissipated in the form of adhesive work and viscous dissipation, so that only a small portion of the energy is converted into kinetic energy. Therefore, the energies during the coalescence process are also analyzed in this paper. Firstly, for the coalescence-induced jumping with two unequal-sized droplets, let the droplet density be ρ, the viscosity is μ, the surface tension is σ_1, and the initial radii of two spherical droplets are R_s with the small one and R_l with the large one, respectively, and the radius ratio is $R^* = R_l/R_s$. The coalesced droplet radius R_c can be computed by

$$R_c = \left(R_s^3 + R_l^3\right)^{\frac{1}{3}}. \tag{3}$$

Assuming that the contact angle between the droplets and the surface is 180 degrees and there is no viscous dissipation, that is, all the surface energy released during the merging process of the two droplets is converted into the kinetic energy of the large droplets after the merging. According to the energy conservation, we have

$$\sigma_1\left(4\pi R_s^2 + 4\pi R_l^2\right) = \sigma_1 4\pi\left(R_s^3 + R_l^3\right)^{\frac{2}{3}} + \frac{1}{2}\left(\frac{4}{3}\pi R_s^3\rho + \frac{4}{3}\pi R_l^3\rho\right){v_j}^2. \tag{4}$$

Therefore, the excess surface energy generated by the merger process can be expressed as

$$\Delta E_s = 4\pi\sigma_1 R_s^2\left[1 + (R^*)^2 - \left(1 + (R^*)^3\right)^{\frac{2}{3}}\right]. \tag{5}$$

According to the viscous dissipation formula [19], the total viscous dissipation of two droplets with unequal radii is derived as

$$\Delta E_{vis} \approx \frac{3}{2}\mu\pi\sqrt{\frac{\sigma_1 R_s^3}{\rho}}[1 + (R^*)^3]^{\frac{3}{2}}. \tag{6}$$

The kinetic energy at the moment of jumping after the coalescence of droplets is defined as

$$E_j = \frac{1}{2}nm_0 v_j^2, \tag{7}$$

where n is the number of atoms, and m_0 is the mass of each argon atom. Therefore, the conversion efficiency of energy is

$$\eta = \frac{E_j}{\Delta E_s}. \quad (8)$$

Therefore, by analyzing the proportion of viscous dissipation to excess surface energy $\Delta E_{vis}/\Delta E_s$, it can be seen that as the radius ratio R* deviates from 1, this proportion rapidly increases, which means viscous dissipation rapidly increases, leading to a rapid decrease in jumping velocity v_j. However, the result calculated by this formula is approximate and cannot be quantitatively analyzed accurately. Thus, it can only obtain the trend of energy changes. In the future, further optimization of the viscous dissipation theory is needed to obtain more accurate results.

The conversion efficiency of energy with radius ratio for three series is shown in Figure 6. It can be seen from this figure the variation trend of conversion efficiency of energy is basically the same as that of jumping velocity with the ratio of two unequal-sized droplets. When the radius ratio is less than 1.3, the conversion efficiency of energy is greater than 1.2%. At this period, inertial capillary force plays a dominant role, and the efficiency conversion is high. When the radius ratio is greater than 1.3, the energy conversion efficiency rapidly decreases to below 1.0%, because viscous force dominates the coalescence and jumping. When the radius ratios reach 2.5, 2.7, and 3.0, respectively, the inertial capillary force has little effect and the energy conversion efficiency is zero, which means the coalesced droplets are no longer jumping and they have reached their critical radius ratios.

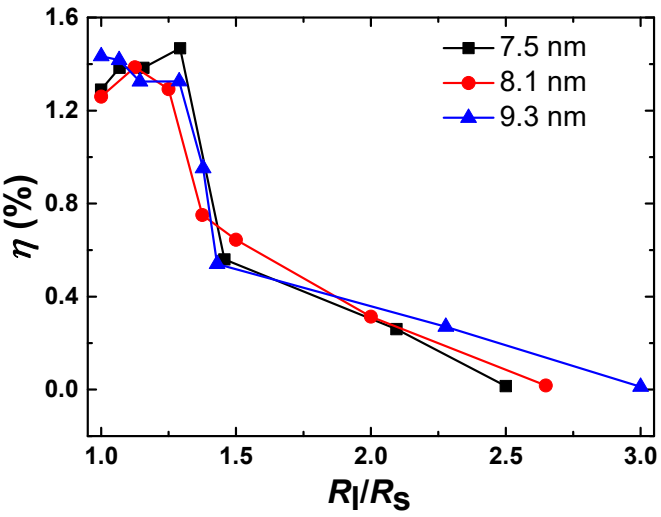

Figure 6. Evolution of conversion rates of energy with radius ratio for three series.

4. Conclusions

The present work investigates coalescence-induced jumping with unequal-sized droplets on superhydrophobic surfaces using molecular dynamic simulations. The radius ratio and the radius of the small droplets are changed to obtain the evolution of velocity and the critical radius ratios for characterizing whether droplets can jump. Thus, the effect of the radius of small droplets on critical radius ratios is revealed for the first time. Additionally, it provides a theoretical reference for the distribution of droplets in condensation heat transfer phenomena. We show that the radius ratio significantly affects jumping velocity. With the same small droplet radius, the slopes of the vertical velocity in the stages of velocity growth and reduction are both gradually decreasing with the increasing radius ratio, and the jumping velocity also decreases accordingly. We can draw the conclusion that there is an optimal radius ratio that can maximize the jumping velocity, while the radius ratio exceeds a certain range, it will suppress the droplet jumping until there is no longer jumping after merging. Subsequently, the critical radius ratios are observed by adjusting the small droplet radius and a series of radius ratios. It is found that the critical radius ratios

are gradually increasing with increasing the radii of small droplets. Furthermore, through analyzing the energy conversion during the coalescence process, it is also revealed that when the radius ratios reach their critical values for the above three series, respectively, the inertial capillary force has little effect and the energy conversion efficiency is zero, causing the coalesced droplets no longer jumping. In general, summarizing the variation of velocity with different radius ratios makes the original chaotic trend is clearly recognized, and the primary reason for whether droplet jumping with different critical radius ratios is revealed.

Author Contributions: Conceptualization, M.-J.L. and F.-F.X.; software, X.-Q.R.; investigation, Z.-H.L.; writing—original draft, M.-J.L.; supervision, W.-P.H. and F.-F.X.; funding acquisition, M.-J.L. and F.-F.X. All authors have read and agreed to the published version of the manuscript.

Funding: This research was funded by NEEPU Scientific Research Foundation for PhDs (BSJXM-12032) and NEEPU Scientific Research Foundation for PhDs (BSJXM-12034).

Data Availability Statement: No new data were created or analyzed in this study. Data sharing is not applicable to this article.

Conflicts of Interest: The authors declare no conflict of interest.

Nomenclature

v^*	dimensionless jumping velocity
v_j	measured jumping velocity, m·s^{-1}
u_{ic}	inertial-capillary velocity, m·s^{-1}
σ_l	surface tension, N·m^{-1}
r	distance between particles, Å
ρ	density, kg·m^{-3}
V_{ij}	potential energy between particles, eV
R	droplet radius, m
σ	particle spacing when the potential is zero, Å
c_{ij}	energy parameter
ε	the minimum value of the potential, meV
T	temperature, K
v_z	vertical velocity, m·s^{-1}
t	time, ps
r_b	width of the liquid bridge, Å
$\Delta\tau$	space of time, ps
C_b	a constant
τ	inertia time, s
R_s	radius of the small droplet, Å
R_l	radius of the large droplet, Å
R_c	radius of the coalesced droplet, Å
μ	viscosity, Pa·s
n	number of atoms
m_0	mass of each argon atom, kg
ΔE_s	excess surface energy, eV
ΔE_{vis}	viscous dissipation, eV
E_j	kinetic energy, eV
η	conversion efficiency of energy

References

1. Edalatpour, M.; Murphy, K.R.; Mukherjee, R.; Boreyko, J.B. Bridging-droplet thermal diodes. *Adv. Funct. Mater.* **2020**, *30*, 2004451. [CrossRef]
2. Foulkes, T.; Sett, S.; Sokalski, P.; Oh, J.; Miljkovic, N. Fundamental limits of jumping droplet heat transfer. *Appl. Phys. Lett.* **2020**, *116*, 093701. [CrossRef]
3. Dalawai, S.P.; Aly, M.A.S.; Latthe, S.S.; Xing, R.M.; Sutar, R.S.; Nagappan, S.; Ha, C.S.; Sadasivuni, K.K.; Liu, S.H. Recent advances in durability of superhydrophobic self-cleaning technology: A critical review. *Prog. Org. Coat.* **2020**, *138*, 105381. [CrossRef]

4. Yu, C.; Sasic, S.; Liu, K.; Salameh, S.; Ras, R.H.A.; Ommen, J.R.V. Nature-inspired self-cleaning surfaces: Mechanisms, modelling, and manufacturing. *Chem. Eng. Res. Des.* **2020**, *155*, 48–65. [CrossRef]
5. Geyer, F.; D'Acunzi, M.; Sharifi-Aghili, A.; Saal, A.; Gao, N.; Kaltbeitze, A.; Sloot, T.F.; Berger, R.; Butt, H.J.; Vollmer, D. When and how self-cleaning of superhydrophobic surfaces works. *Sci. Adv.* **2020**, *6*, 9727. [CrossRef]
6. Feng, C.; Zhang, Z.; Li, J.; Qu, Y.; Xing, D.D.; Gao, X.F.; Zhang, Z.Y.; Wen, Y.H.; Ma, Y.J.; Ye, J.J.; et al. A bioinspired, highly transparent surface with dry-style antifogging, antifrosting, antifouling, and moisture self-cleaning properties. *Macromol. Rapid Commun.* **2018**, *40*, 1800708. [CrossRef] [PubMed]
7. Zhao, G.; Zou, G.; Wang, W.; Geng, R.K.; Yan, X.; He, Z.Y.; Liu, L.; Zhou, X.; Lv, J.Y.; Wang, J.J. Rationally designed surface microstructural features for enhanced droplet jumping and anti-frosting performance. *Soft Matter* **2020**, *16*, 4462–4476. [CrossRef] [PubMed]
8. Zhao, G.; Zou, G.; Wang, W.; Geng, R.K.; Yan, X.; He, Z.Y.; Liu, L.; Zhou, X.; Lv, J.Y.; Wang, J.J. Competing effects between condensation and self-removal of water droplets determine antifrosting performance of superhydrophobic surfaces. *ACS Appl. Mater. Interfaces* **2020**, *12*, 7805–7814. [CrossRef] [PubMed]
9. Boreyko, J.B.; Chen, C.-H. Self-propelled dropwise condensate on superhydrophobic surfaces. *Phys. Rev. Lett.* **2009**, *103*, 184501. [CrossRef]
10. Ölçeroğlu, E.; Hsieh, C.Y.; Rahman, M.M.; Lau, K.K.S.; McCarthy, M. Full-field dynamic characterization of superhydrophobic condensation on biotemplated nanostructured surfaces. *Langmuir* **2014**, *30*, 7556–7566. [CrossRef]
11. Li, G.; Alhosani, M.H.; Yuan, S.; Liu, H.R.; Ghaferi, A.A.; Zhang, T.J. Microscopic droplet formation and energy transport analysis of condensation on scalable superhydrophobic nanostructured copper oxide surfaces. *Langmuir* **2014**, *30*, 14498–14511. [CrossRef]
12. Xie, J.; Xu, J.; Shang, W.; Zhang, K. Dropwise condensation on superhydrophobic nanostructure surface, part II: Mathematical model. *Int. J. Heat Mass Transf.* **2018**, *127*, 1170–1187. [CrossRef]
13. Hou, Y.M.; Yu, M.; Chen, X.M.; Wang, Z.K.; Yao, S.H. Recurrent filmwise and dropwise condensation on a beetle mimetic surface. *ACS Nano* **2015**, *9*, 71–81. [CrossRef]
14. Miljkovic, N.; Wang, E.N. Condensation heat transfer on superhydrophobic surfaces. *MRS Bull.* **2013**, *38*, 397–406. [CrossRef]
15. Miljkovic, N.; Enright, R.; Nam, Y.; Lopez, K.; Dou, N.; Sack, J.; Wang, E.N. Jumping-droplet-enhanced condensation on scalable superhydrophobic nanostructured surfaces. *Nano Lett.* **2013**, *13*, 179–187. [CrossRef]
16. Liu, F.J.; Ghigliotti, G.; Feng, J.J.; Chen, C.H. Numerical simulations of self-propelled jumping upon drop coalescence on non-wetting surfaces. *J. Fluid Mech.* **2014**, *752*, 39–65. [CrossRef]
17. Wang, F.-C.; Yang, F.; Zhao, Y.-P. Size effect on the coalescence-induced self-propelled droplet. *Appl. Phys. Lett.* **2011**, *98*, 053112. [CrossRef]
18. Peng, B.L.; Wang, S.F.; Lan, Z.; Xu, W.; Wen, R.F.; Ma, X.H. Analysis of droplet jumping phenomenon with lattice Boltzmann simulation of droplet coalescence. *Appl. Phys. Lett.* **2013**, *102*, 151601.
19. Lv, C.J.; Hao, P.F.; Yao, Z.H.; Song, Y.; Zhang, X.W.; He, F. Condensation and jumping relay of droplets on lotus leaf. *Appl. Phys. Lett.* **2013**, *103*, 021601. [CrossRef]
20. Farokhirad, S.; Morris, J.F.; Lee, T. Coalescence-induced jumping of droplet: Inertia and viscosity effects. *Phys. Fluids* **2015**, *27*, 102102. [CrossRef]
21. Liu, X.L.; Cheng, P.; Quan, X.J. Lattice Boltzmann simulations for self-propelled jumping of droplets after coalescence on a superhydrophobic surface. *Int. J. Heat Mass Transf.* **2014**, *73*, 195–200. [CrossRef]
22. Attarzadeh, R.; Dolatabadi, A. Coalescence-induced jumping of micro-droplets on heterogeneous superhydrophobic surfaces. *Phys. Fluids* **2017**, *29*, 012104. [CrossRef]
23. Liang, Z.; Keblinski, P. Coalescence-induced jumping of nanoscale droplets on super-hydrophobic surfaces. *Appl. Phys. Lett.* **2015**, *107*, 143105. [CrossRef]
24. Xie, F.F.; Lu, G.; Wang, X.D.; Wang, B.B. Coalescence-induced jumping of two unequal sized nanodroplets. *Langmuir* **2018**, *34*, 2734–2740. [CrossRef] [PubMed]
25. Enright, R.; Miljkovic, N.; Sprittles, J.; Nolan, K.; Mitchell, R.; Wang, E.N. How coalescing droplets jump. *ACS Nano* **2014**, *8*, 10352–10362. [CrossRef]
26. Liu, T.Q.; Sun, W.; Sun, X.Y.; Ai, H.R. Mechanism study of condensed drops jumping on super-hydrophobic surfaces. *Colloids Surf. A* **2012**, *414*, 366–374. [CrossRef]
27. Foiles, S.M.; Baskes, M.I.; Daw, M.S. Embedded-atom-method functions for the fcc metals Cu, Ag, Au, Ni, Pd, Pt, and their alloys. *Phys. Rev. B* **1986**, *33*, 7983–7991. [CrossRef]
28. Pothier, J.C.; Lewis, L.J. Molecular-dynamics Study of the Viscous to Inertial Crossover in Nanodroplet Coalescence. *Phys. Rev. B* **2012**, *85*, 115447. [CrossRef]
29. Eggers, J.; Lister, J.R.; Stone, H.A. Coalescence of Liquid Drops. *J. Fluid Mech.* **1999**, *401*, 293–310. [CrossRef]